

Organogels with Fe(III) Complexes of Phosphorus-Containing Amphiphiles as Two-Component Isothermal Gelators

Mathew George,^{†,||} Gary P. Funkhouser,[‡] Pierre Terech,[§] and Richard G. Weiss^{*,†}

Department of Chemistry, Georgetown University, Washington, DC 20057-1227, Halliburton Energy Services, Inc., Duncan, Oklahoma 73533, and Laboratoire Physico-Chimie Moléculaire, CEA-UMR5819, 17 rue des Martyrs, 38054 Grenoble Cedex 9, France

Received April 17, 2006. In Final Form: June 19, 2006

The properties of thermally reversible organogels in which the gelators consist of a phosphonic acid monoester, phosphonic acid, or phosphoric acid monoester and a ferric salt are probed by IR and NMR spectroscopies, optical microscopy, X-ray diffraction, rheology, and light and small-angle neutron scattering (SANS) techniques. This is one of a small number of two-component molecular gelator systems in which gelation can be induced isothermally. The data indicate that complexation between the phosphonate moieties and Fe(III) is accompanied by their in situ polymerization to form self-assembled fibrillar networks that encapsulate and immobilize macroscopically the organic liquid component. From SANS measurements, the cross-sectional radii of the cylindrical fibers are ca. 15 Å. The efficiencies of the gelators (based on the diversity of the liquids gelled, the minimum concentration of gelator required to make a gel at room temperature, and the temporal and thermal stabilities of the gels) have been determined. With a common ferric salt and liquid component, phosphonic acid monoesters are generally more efficient than phosphinic acids or phosphoric acid esters. Of the phosphonic acid monoesters, monophosphonates are better gelator components than bisphosphonates, and introduction of an ω -hydroxy group on the alkyl chain directly attached to phosphorus reduces significantly gelation ability. Several of the gels are stable for very long periods at room temperature. When heated, they revert to sols over wide temperature ranges. The structures of the gelator complexes and the mechanism of their formation and transformation to gels in selected liquids are examined as well.

Introduction

Organic–inorganic hybrid materials have received increased attention in recent years due to their processability and properties that can differ enormously from those of their separate parts.^{1,2} Examples of such hybrids include covalently linked or coordination polymers formed by metal ions interconnected through organic ligands,³ polyhedral oligomeric silsesquioxanes,⁴ layered nanocomposites,⁵ and polymer–silica gel composites.⁶ Solutions of several organic molecules aggregate into elongated objects resembling inverted giant wormlike micelles⁷ and become gels⁸

when complexed with Al(III)^{9,10} or Fe(III) and other transition metals.^{11,12} Their entangled networks immobilize the liquid component through capillary forces and surface tension.^{8a,c}

Complexes between metal ions and several types of phosphorus-containing molecules have found uses as flame retardants¹³ and adhesives to metals, bone, and dentin,¹⁴ selective binders to metals,¹⁵ hydraulic fracturing agents,¹⁶ liquid crystals,¹⁷ optical

* Author for correspondence. E-mail: weissr@georgetown.edu.

[†] Georgetown University.

[‡] Halliburton Energy Services, Inc.

[§] CEA-UMR5819.

^{||} Current address: Sepax Technologies, Inc., Newark, DE.

(1) (a) Nalwa, H. S., Ed. *Handbook of Organic–Inorganic Hybrid Materials and Nanocomposites*; American Scientific Publishers: Stevenson Ranch, CA, 2003. (b) Pyun, J.; Xia, J.; Matyjaszewski, K. *Synthesis and Properties of Silicones and Silicone-Modified Materials* (ACS Symposium Series 838); American Chemical Society: Washington, DC, 2003; pp 273–284.

(2) (a) Walcarius, A. *Chem. Mater.* **2001**, *13*, 3351–3372. (b) Cerveau, G.; Corriu, R. J. P.; Framery, E. *Chem. Mater.* **2001**, *13*, 3373–3388. (c) Pyun, J.; Matyjaszewski, K. *Chem. Mater.* **2001**, *13*, 3436–3448. (d) Mitzi, D. B. *Chem. Mater.* **2001**, *13*, 3283–3298. (e) Guizard, C.; Bac, A.; Barboiu, M.; Hovnanian, N. *Mol. Cryst. Liq. Cryst.* **2000**, *354*, 91–106. (f) Schmidt, H. K.; Mennig, M.; Noninger, R.; Oliveira, P. W.; Schirra, H. *Mater. Res. Soc. Symp. Proc.* **1999**, *576*, 395–407. (g) Hagrman, P. J.; Hagrman, D.; Zubieta, J. *Angew. Chem., Int. Ed.* **1999**, *38*, 2639–2684. (h) Seddon, A. B. *Critical Rev. Opt. Sci. Technol.* **1997**, *CR68*, 143–171. (i) Chujo, Y. *Curr. Opin. Solid State Mater. Sci.* **1996**, *1*, 806–811. (j) Schubert, U. *New J. Chem.* **1994**, *18*, 1049–1058. (k) Dong, S.; Chen, X. *J. Biotechnol.* **2002**, *82*, 303–323.

(3) Bolck, B. P. In *Inorganic Polymers*; Stone, F. G. A., Graham, W. A. G., Eds.; Academic Press: London, 1962; p 447.

(4) (a) Kim, K.-M.; Chujo, Y. *J. Mater. Chem.* **2003**, *13*, 1384–1391. (b) Provatas, A.; Matisons, J. G. *Trends Polym. Sci.* **1997**, *5*, 327–332. (c) Laine, R. M.; Zhang, C.; Sellinger, A.; Viculis, L. *Appl. Organomet. Chem.* **1998**, *12*, 715–723.

(5) (a) Krishnamoorti, R.; Vaia, R. A.; Giannelis, E. P. *Chem. Mater.* **1996**, *8*, 1728–1734. (b) Weimer, M. W.; Chen, H.; Giannelis, E. P.; Sogah, D. Y. *J. Am. Chem. Soc.* **1999**, *121*, 1615–1616.

(6) (a) Mascia, L. *Trends Polym. Sci.* **1995**, *3*, 61–66. (b) Novak, B. M. *Adv. Mater.* **1993**, *5*, 422–433.

(7) (a) Lequeux, F.; Candau, S. J. In *Theoretical Challenges in the Dynamics of Complex Fluids* (NATO ASI Series, Series E); McLeish, T., Ed.; Kluwer Academic: Dordrecht, 1997; Vol. 339, p 181. (b) van der Schoot, P.; Wittmer, J. P. *Macromol. Theory Simul.* **1999**, *8*, 428–432. (c) Aliotta, F. *Trends Phys. Chem.* **1997**, *6*, 31–53.

(8) (a) Terech, P.; Weiss, R. G. *Chem. Rev.* **1997**, *97*, 3133–3159. (b) Abdallah, D. J.; Weiss, R. G. *Adv. Mater.* **2000**, *12*, 1237–1247. (c) Weiss, R. G.; Terech, P., Eds.; *Molecular Gels. Materials with Self-Assembled Fibrillar Networks*; Springer: Dordrecht, 2005. (d) Terech, P.; Weiss, R. G. In *Surface Characterization Methods*; Milling, A. J., Ed.; Marcel Dekker: New York, 1999; Chapter 10. (e) George, M.; Weiss, R. G. *Acc. Chem. Res.* in press.

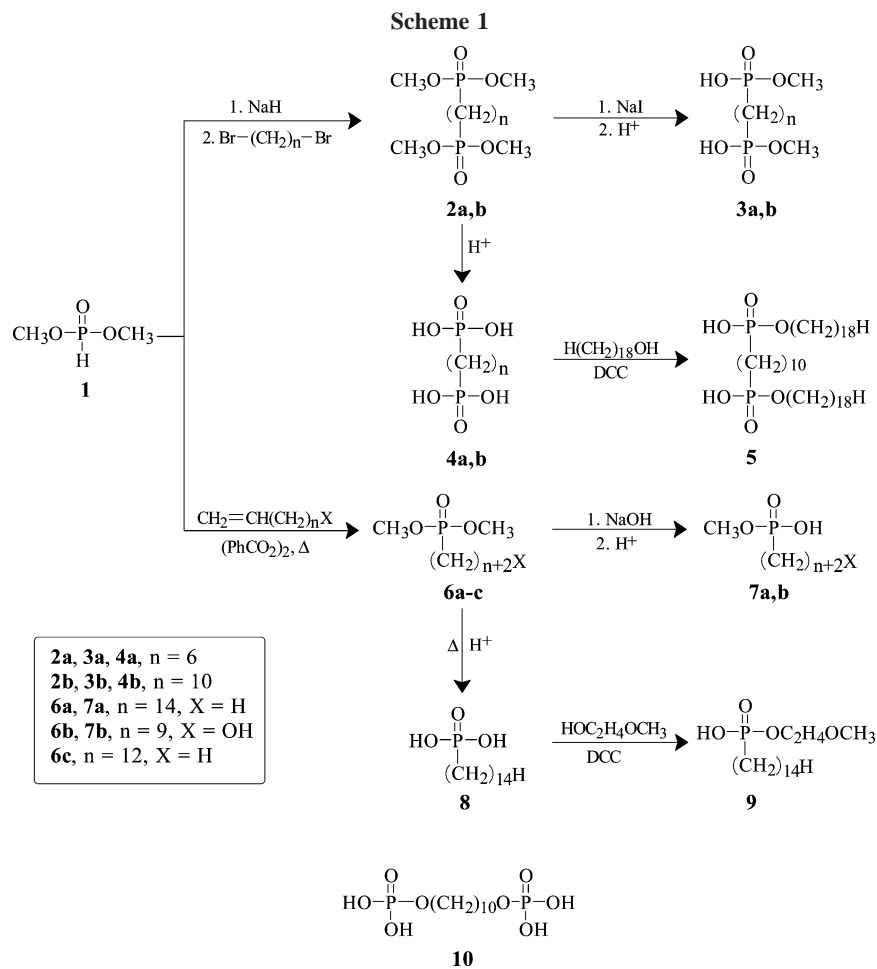
(9) (a) Montagne, L.; Palavit, G.; Draoui, M. *J. Non-Cryst. Solids* **1993**, *155*, 115–121. (b) Fukasawa, J.; Tsutsumi, H.; Ishida, A. *Cosmet. Toiletries* **1988**, *103*, 78–80. (c) Fukasawa, J.; Tsutsumi, H.; Ishida, A. *Int. J. Cosmet. Sci.* **1989**, *11*, 153–165. (d) Arbuthnot, D.; Wang, X.-j.; Knobbe, E. T. *Mater. Res. Soc. Symp. Proc.* **1994**, *346*, 569–578. (e) Boulton, J. M.; Jones, K.; Emblem, H. G. *J. Mater. Sci.* **1989**, *24*, 979–990. (f) Seely, G. R.; Hart, R. L. *Macromolecules* **1976**, *9*, 483–489. (g) Flagg, E. E.; Schmidt, D. L. *J. Am. Chem. Soc.* **1968**, *90*, 4173–4174.

(10) (a) Markovic, N.; Dutta, N. K.; Williams, D. R. G.; Matisons, J. In *Polymer Gels: Fundamentals and Applications* (ACS Symp. Ser. 833); Bohidar, H. B., Dubin, P., Osada, Y., Eds.; American Chemical Society: Washington, DC, 2003; pp 190–204. (b) Friberg, S. *Acta Chim. Scand.* **1966**, *20*, 901. (c) Fieser, L. F.; Harris, G. C.; Hershberg, E. B.; Morgana, M.; Novello, F. C.; Putnam, S. T. *J. Ind. Eng. Chem.* **1946**, *38*, 768–773.

(11) (a) Ogoshi, T.; Itoh, H.; Kim, K.-M.; Chujo, Y. *Polym. J.* **2003**, *35*, 178–184. (b) Singh, D. K.; Garg, S. K.; Bharadwaj, R. K. *Res. J. Chem. Environ.* **1999**, *3*, 53–59. (c) Sohna, J.-E. S.; Fages, F. *Chem. Commun.* **1997**, 327–328. (d) Linden, L. A.; Rabek, J. F. *J. Appl. Polym. Sci.* **1993**, *50*, 1331–1341. (e) Chujo, Y.; Sada, K.; Saegusa, T. *Macromolecules* **1993**, *26*, 6315–6319.

(12) (a) Crescenzi, V.; Giancotti, V.; Ripamonti, A. *J. Am. Chem. Soc.* **1965**, *87*, 391–392. (b) Brena, B. M.; Ryden, L. G.; Porath, J. *Biotech. Appl. Biochem.* **1994**, *19*, 217–231. (c) Chujo, Y.; Sada, K.; Saegusa, T. *Polym. J.* **1993**, *25*, 599–608. (d) Terech, P.; Schaffhauser, V.; Maldivi, P.; Guenet, J. M. *Eur. Polym. Lett.* **1992**, *17*, 515–521. (e) Terech, P.; Schaffhauser, V.; Maldivi, P.; Guenet, J. M. *Langmuir* **1992**, *8*, 2104–2106.

(13) Lindsay, C.; Hill, S.; Hearn, M.; Manton, G.; Everall, N.; Bunn, A.; Heron, J.; Fletcher, I. *Polym. Int.* **2000**, *49*, 1183–1192.



materials,¹⁸ and components in cosmetics.^{9b} Also, several phosphorus-containing chemical warfare agents are known to be deactivated by complexation with metal ions.¹⁹ To the best of our knowledge, their application in gel form has not been explored although it may have advantages over other formulations.

Here, the gelating abilities of solutions of bisphosphonate esters (**3a,b** and **5**), phosphonic acids (**4a,b**), monophosphonate esters (**7a,b** and **9**), and a phosphoric acid ester (**10**) (Scheme 1), when complexed in situ by MO-86, a commercial product containing an aqueous solution of Fe(III) sulfate and dibutylaminoethanol,²⁰ have been studied. These gelators are one of the relatively few known classes of two-component systems.^{21,22} They allow gelation isothermally, based on in situ molecular interactions between the phosphorus-containing "latent" gelator and Fe(III) ions that lead to linear aggregation in the form of giant inverted

micellar rods. This is an example of macrogelation triggered by molecular chemistry events.

Each of the esters has one or more long alkyl chains to increase its solubility in a variety of common organic liquids. We find that the gelation efficiencies depend mainly on the nature of the substituents attached to the phosphorus atom and that the time required for the self-assembled fibrillar network (SAFIN) of the gel phase to be established can be controlled by varying the liquid component and the spacer length of bisphosphonates. In toto, the results provide insights into the structural features that lead to successful two-component gelators of this type and a comprehensive picture of the structures of their isothermally formed gels.

Experimental Section

Instrumentation. Melting points (corrected) were measured and optical micrographs were observed on samples between glass cover slips using a Leitz 585 SM-LUX-POL microscope equipped with

(14) (a) Sawada, K.; Duan, W.; Ono, M.; Satoh, K. *J. Chem. Soc., Dalton Trans.* **2000**, 919–924. (b) Ceconi, F.; Ghilardi, C.; Luis, P.; Midollini, S.; Orlandini, A.; Dakternieks, D.; Duthie, A.; Dominguez, S.; Berti, E.; Vacca, A. *J. Chem. Soc., Dalton Trans.* **2001**, 211–217. (c) Moszner, N.; Zeuner, F.; Fischer, U. K.; Rheinberger, V. *Macromol. Chem. Phys.* **1999**, *200*, 1062–1067. (d) Moszner, N.; Zeuner, F.; Pfeiffer, S.; Schurte, I.; Rheinberger, V.; Drache, M. *Macromol. Mater. Eng.* **2001**, *286*, 225–231.

(15) (a) Cabasso, I.; Smid, J.; Sahni, S. K. *J. Appl. Polym. Sci.* **1990**, *41*, 3025–3042. (b) Riedelsberger, K.; Jaeger, W.; Friedrich, A. *Des. Mon. Polym.* **2000**, *3*, 35–53.

(16) (a) Monroe, R. F.; Rooker, B. E. U.S. Patent 3,494,949, 1970. *Chem. Abstr.* **1970**, *72*, 81204. (b) Monroe, R. F. U.S. 3,505,374, 1970. *Chem. Abstr.* **1970**, *73*, 5761. (c) Kim, V.; Bazhenov, A. V.; Kienskaya, K. I. *Colloid J.* **1997**, *59*, 455–460.

(17) Fukasawa, J.-I.; Tsutsumi, H. *J. Colloid Interface Sci.* **1991**, *143*, 69–76.

(18) Hayashi, N.; Mizusawa, S.; Koizumi, T.; Machida, K. Eur. Pat. # EP 2001–307186, 2002.

(19) Wagner, G. W.; Procell, L. R.; O'Connor, R. J.; Munavalli, S.; Carnes, C. L.; Kapoor, P. N.; Klabunde, K. J. *J. Am. Chem. Soc.* **2001**, *123*, 1636–1644.

(20) Geib, G. G. U.S. Patent 6,342,468 B1, 2000. *Chem. Abstr.* **2000**, *133*, 364314.

(21) (a) George, M.; Weiss, R. G. *J. Am. Chem. Soc.* **2001**, *123*, 10393–10394. (b) George, M.; Weiss, R. G. *Langmuir* **2002**, *18*, 7124–7135. (c) George, M.; Weiss, R. G. *Langmuir* **2003**, *19*, 1017–1025.

(22) (a) Wang, C.; Robertson, A.; Weiss, R. G. *Langmuir* **2003**, *19*, 1036–1046. (b) Bauer, T.; Thomann, R.; Muelhaupt, R. *Macromolecules* **1998**, *31*, 7651–7658. (c) Pozzo, J. L.; Clavier, G.; Rustemeyer, F.; Bouas-Laurent, H. *Mol. Cryst. Liq. Cryst.* **2000**, *344*, 101–106. (d) Rizkov, D.; Gun, J.; Lev, O.; Sicsic, R.; Melman, A. *Langmuir* **2005**, *21*, 12130–12138. (e) Bao, C.; Lu, R.; Jin, M.; Xue, P.; Tan, C.; Liu, G.; Zhao, Y. *Org. Biomol. Chem.* **2005**, *3*, 2508–2512. (f) Singh, M.; Tan, G.; Agarwal, V.; Fritz, G.; Maskos, K.; Bose, A.; John, V.; McPherson, G. *Langmuir* **2004**, *20*, 7392–7398. (g) Babu, P.; Sangeetha, N. M.; Vijaykumar, P.; Maitra, U.; Rissanen, K.; Raju, A. R. *Chem. Eur. J.* **2003**, *9*, 1922–1932. (h) Koshima, H.; Matsusaka, W.; Yu, H. *J. Photochem. Photobiol. A: Chem.* **2003**, *156*, 83–90. (i) Friggeri, A.; Gronwald, O.; van Bommel, K. J. C.; Shinkai, S.; Reinhoudt, D. N. *J. Am. Chem. Soc.* **2002**, *124*, 10754–10758. (j) Willemen, H. M.; Vermonden, T.; Marcelis, A. T. M.; Sudhoelter, E. J. R. *Langmuir* **2002**, *18*, 7102–7106. (k) Page, M. G.; Warr, G. G. *J. Phys. Chem. B* **2004**, *108*, 16983–16989.

crossed polars, a Leitz 350 heating stage, and an Omega HH503 microprocessor thermometer connected to a J-K-T thermocouple. IR spectra were obtained on a Perkin-Elmer Spectrum One FT-IR spectrometer interfaced to a computer. NMR spectra were recorded on a Varian 300 MHz spectrometer interfaced to a Sparc UNIX computer using Mercury software. ^1H spectra were referenced to internal TMS, and ^{31}P spectra (H-decoupled) were referenced to the peak from concentrated phosphoric acid (in a sealed inner tube). X-ray diffraction (XRD) of samples in thin, sealed capillaries (0.5 mm diam; W. Müller, Schönwalde, FRG) was performed on a Rigaku R-Axis image plate system with Cu $K\alpha$ X-rays ($\lambda = 1.54056 \text{ \AA}$) generated with a Rigaku generator operating at 46 kV and 46 mA. Data processing and analyses were performed using Materials Data JADE (version 5.0.35) XRD pattern processing software.²³ Molecular calculations of lowest-energy conformations and molecular dimensions used the semiempirical Parametric Method 3 (PM3)²⁴ of the HYPERCHEM package, release 7.1 Pro for Windows from Hypercube, Inc.

Light scattering measurements were performed using a Photon Technology International fluorimeter (Lawrenceville, NJ) with a continuous-wave 75-W xenon lamp as the excitation source. The instrument was controlled by a computer using Felix32 software (ver.1.1, release 2003). Differential scanning calorimetry (DSC) measurements were conducted using a TA Instruments DSC2920 Modulated DSC instrument and samples in crimp-sealed aluminum pans. The rates of heating and cooling were both $10 \text{ }^\circ\text{C}/\text{min}$.

Rheology measurements were made with a Haake RheoStress RS150 stress-controlled rheometer fitted with a 60 mm diameter, 2° titanium cone and plate. The sample was loaded onto the rheometer at $35 \text{ }^\circ\text{C}$ and then cooled to the test temperature of $25 \text{ }^\circ\text{C}$. Constant frequency (1 Hz) oscillatory stress sweeps from 0.05 to 100 or 0.1 to 1000 Pa, depending on the strength of the gel, were performed to obtain the storage modulus and loss modulus. The frequency sweep was obtained at a constant stress of 0.5 Pa that resulted in small strains ($<0.2\%$), well within the linear viscoelastic region determined by the stress sweep.

Small angle neutron diffraction (SANS) measurements were made on the low-angle diffractometer NG7 beam line at the National Institute of Standards and Technology (NIST, Gaithersburg, MD)²⁵ with neutrons of $\lambda = 8.09 \text{ \AA}$ and at detector distances of 15.3, 5.0, and 1.0 m with a detector lateral offset of 0.25 m for the 5.0 and 1.0 m distances. Since the scattering of all gels was isotropic, circular radial averaging was used to extract I versus Q curves. The scattering vector range investigated was $0.0011 < |Q| < 0.33 \text{ \AA}^{-1}$ ($|Q| = 4\pi/\lambda \sin \theta/2$, where θ is the scattering angle and λ is the wavelength of the neutrons). Gels for SANS investigations were prepared with perdeuterated solvents in closed 2 mm path length Suprasil quartz cells.

Materials. Spectroscopic and other characterization data for all new compounds are collected in the Supporting Information. Solvents for syntheses were reagent grade (Aldrich) and dried by standard procedures. Dimethyl phosphite (98%), 1,10-dibromodecane (97%), sodium iodide (reagent grade), 1,10-decanediol (98%), dicyclohexylcarbodiimide (DCC) (99%), 1,6-dibromohexane (96%), 11-hydroxy-1-undecene (98%), benzoyl peroxide (97%), and sodium hydride (60% dispersion in mineral oil) were from Aldrich and used as received. Phosphorus oxychloride (POCl_3) from Fisher Scientific was distilled prior to use. MO-86²⁰ was supplied by Halliburton Energy Services. Perdeuterated solvents used for SANS studies were purchased from Aldrich (toluene- d_8 and D_2O) and CDN Isotopes (n -dodecane- d_{26}).

General Procedure for the Synthesis of Bisphosphonate Esters (3a,b). Under a nitrogen atmosphere, dimethyl phosphite (4 g, 36 mmol) in dry THF (20 mL) was added slowly to a suspension of NaH (36 mmol) in dry THF (20 mL), and the mixture was stirred for 1 h.²⁶ Then, a α,ω -dibromoalkane (12 mmol) in dry THF (20

mL) was added over 30 min, and stirring was continued for an additional 2 h, during which time a white precipitate formed. Finally, the mixture was refluxed for 6 h. The solid was removed by filtration, and the filtrate was concentrated to give a viscous oil (**2a,b**). Unreacted starting material was removed by distillation under reduced pressure, and the residue was purified by silica gel chromatography using 4:1 ethyl acetate:hexane as eluent or by recrystallization from hexane.

Tetraesters, **2a** and **2b**, were partially dealkylated to produce the corresponding diester sodium salts, which were subsequently protonated by bubbling dry HCl gas. In a typical procedure, **2a** (2.25 g, 7.4 mmol) was dissolved in 2-butanone (50 mL). NaI (2.23 g, 14.8 mmol) was added, and the mixture was refluxed for 12 h. The precipitate was separated by filtration and washed with acetone to yield 1.87 g (79%) of the sodium salt.²⁷ The salt was dissolved in methanol (50 mL) and cooled in an ice bath, and dry HCl gas (produced by reacting ammonium chloride with concentrated H_2SO_4 and passing the gas through concentrated H_2SO_4) was passed through for 15 min. The mixture was filtered and an equal amount of ethyl acetate was added to the filtrate. On cooling to ca. $-5 \text{ }^\circ\text{C}$, 1.45 g (90%) of **3a**, mp $109.4\text{--}110.3 \text{ }^\circ\text{C}$, crystallized.

Phosphonic acids **4a,b** were prepared by the complete hydrolyses of **2a,b**. A mixture of **2a** or **2b** (10 mmol) and 6 M hydrochloric acid (20 mL) was refluxed for 4 h.²⁸ The reaction mixture was cooled to room temperature and the solvent was coevaporated with ethanol ($3 \times 50 \text{ mL}$). The residue was purified by recrystallization from 1:4 methanol:ethyl acetate.

Synthesis of 5. Under a nitrogen atmosphere, DCC (1.65 g, 8 mmol) in dry THF (30 mL) was added over 1 h to a refluxing solution of phosphonic acid **4b** (1.0 g, 3.3 mmol) and 1-octadecanol (2.0 g, 7.4 mmol).²⁹ The mixture was refluxed for an additional 12 h, during which time a white solid (1,3-dicyclohexylurea) precipitated. The mixture was filtered, and the filtrate was concentrated under reduced pressure. The resulting mixture was dissolved in 1 N NH_4OH , neutralized with 6 M HCl, and extracted with 1:1 ethyl acetate:chloroform. The organic extract was concentrated, and the product was recrystallized from chloroform to yield 1.87 g (66%) of **5**.

Compounds **6a–c** were prepared from **1** and an alkene by a procedure adapted from the literature³⁰ using benzoyl peroxide as the free radical initiator and $80\text{--}90 \text{ }^\circ\text{C}$ as the temperature. Excess **1** was removed by distillation under reduced pressure and the intermediate dimethyl esters (**6a–c**) were used without further purification for the preparation of **7a,b**.³⁰

Monophosphonic acid **8** was prepared by the complete hydrolysis of **6c** in acidic media using the conditions described above for **4a,b**. Compound **9** was prepared by the reaction of **8** with ethylene glycol monomethyl ether in the presence of DCC by a procedure similar to that for **5**.

Synthesis of 10. Compound **10** was synthesized by a procedure reported for similar compounds.³¹ 1,10-Decanediol (6.74 g, 38.7 mmol) was added to a solution of POCl_3 (16.4 g, 107 mmol) in dry toluene (100 mL), and the mixture was heated to ca. $105 \text{ }^\circ\text{C}$ for 6 h and then concentrated to residue. The residue was dissolved in toluene (100 mL) and reduced again to a residue that was added to water (200 mL) and refluxed for 3 h. After removal of the water on a rotary evaporator, 100 mL of ethanol was added to the residue, and it was reduced to a residue. This procedure was repeated 3 times. The residue was dissolved in 1:4 methanol:ethyl acetate, and the solution was cooled in a freezer. The white solid was filtered and dried to yield 9.5 g (73%) of **10**, mp $125.5\text{--}127.0 \text{ }^\circ\text{C}$.

Preparation of 7a/MO-86 Complex for SANS and XRD Studies. **7a** (640 mg, 2 mmol) was stirred and warmed in pentane

(27) Boutevin, B.; Hervaud, Y.; Jeanmaire, T.; Boulahna, A.; Elasri, M. *Phosphorus Sulfur Silicon Relat. Elem.* **2001**, *174*, 1–14.

(28) For the synthesis of a similar compound, see: Cavalier, J.-F.; Ransac, S.; Verger, R.; Buono, G. *Chem. Phys. Lipids* **1999**, *100*, 3–31.

(29) Burger, A.; Anderson, J. J. *J. Am. Chem. Soc.* **1957**, *79*, 3575–3579.

(30) (a) Taylor, R. S.; Funkhouser, G. P. US Patent 6,511,944 B2, 2003. (b) Taylor, R. S.; Funkhouser, G. P. Eur. Pat. #EP 1236863, 2002. (c) Funkhouser, G. P.; Taylor, R. S. High-Performance Organogelators with Improved Thermal Stability and a Reduced Tendency for Crude Distillation Tower Fouling. paper No. 22 presented at the Tekna 2004 International Oil Field Chemistry Symposium, Geilo, Norway, March 28–31, 2004.

(23) Materials Data Inc., Release 5.0.35 (SPS), Livermore, California.

(24) Stewart, J. J. P. *J. Comput. Chem.* **1989**, *10*, 209–220.

(25) Glinka, C. J.; Barker, J. G.; Hammouda, B.; Krueger, S.; Moyer, J. J.; Orts, W. J. *J. Appl. Crystallogr.* **1998**, *31*, 430–445.

(26) Kim, D. Y.; Kong, M. S. *J. Chem. Soc., Perkin Trans. 1* **1994**, 3359–3360.

Table 1. Gelation Properties of Complexes of 2 wt % **3-5**, **7a**, or **10** and Equal Weights of MO-86 in Various Liquids^a

liquid	3a	3b	4a	4b	5	7a	10
hexane	I	I	I	I	P	CG ^d (76–87)	I
<i>n</i> -octane	I	I	I	I	P + VS	CG ^d (56–82)	I
silicone oil	I	I	I	I	jelly	TG ^d (33–39)	I
ethanol	P/aggr	aggr	OG ^e (28)	P/jelly	I	P	jelly
1-butanol	aggr	jelly	jelly	jelly	P/aggr	P	jelly
1-octanol	jelly	P + VS	P	P	P + VS	P	P + VS
benzyl alcohol	VS	jelly ^c	P	jelly	TG ^f (95–113)	P + VS	microcrystallites
DMSO	jelly ^b	CG ^d (115–150)	S	S	P + VS	P	S
toluene	I	I	I	I	TG ^c (72–94)	TG ^d (50–62)	I
PhCl	I	I	I	I	TG ^d (112–135)	TG ^d (28–35)	I
CCl ₄	I	I	I	I	TG ^d (94–130)	TG ^d (78–86)	I
water	I	I	P	P/aggr	I	I	P

^a T_g (°C) ranges are in parentheses. S, solution; P, precipitate; I, insoluble; CG, clear gel; TG, turbid gel; OG, opaque gel; VS, viscous solution.

^b Changed to CG after 5 weeks ($T_g = 110–150$ °C). ^c Became a partial gel after 5 weeks. Stable at room temperature in a sealed vial for: ^d > 2 years;

^e 1 month; ^f 5 weeks.

(50 mL) until it dissolved. MO-86 (0.5 mL, 0.68 g) was added with vigorous mechanical stirring, and a strong gel formed within a few minutes. Pentane was removed by passing a stream of nitrogen over the gel as it was warmed on a hot plate. The resulting solid was dried for 3 days under house vacuum over phosphorus pentoxide and then ground into a powder.

Light Scattering Studies. Solutions of 2 wt % **3b** in DMSO and 2 wt % **7a** in *n*-octane were prepared and placed in 1 cm × 1 cm quartz cuvettes. Ca. 2 vol % MO-86 was added with shaking for ca. 10 s, and the scattering intensity was recorded at 470 nm as a function of time. Scattering from the quartz cuvette, solvent, and the solution before adding MO-86 was negligible compared to that obtained after adding MO-86.

Gelation Studies. A weighed amount of liquid was placed in a glass tube (10 mm i.d.) containing a known amount of phosphorus-containing reagent. The tube was heated in an oil bath until the solid dissolved completely. Then, a weighed aliquot of MO-86 was added at ca. 90 °C, and the mixture was shaken for a few minutes. The mixture was inverted and examined visually after cooling it to ambient temperature.

Measurement of Gelation Temperature (T_g). Gelation temperatures were determined by the inverse flow method.³² A gel in a flame-sealed glass tube was inverted, strapped to a thermometer near the bulb, and immersed in a stirred oil bath at room temperature. The temperature of the bath was raised slowly, and the range of T_g was taken from the points at which the first part of the gel fell until all had fallen.

Results and Discussion

Gelation Studies. Unless stated otherwise, complexes were made in situ from a phosphorus-containing molecule dissolved in a liquid of interest. Results from gelation experiments with ca. 2 wt % of a bolaamphiphile, **3–5** or **10**, or the monophosphonate ester **7a** and an almost equal weight of MO-86 in different liquids are summarized in Table 1. Whereas the monophosphonate ester **7a**/Fe(III) complex was able to gelate low polarity liquids efficiently, the complexed bolaamphiphiles, except **5**/Fe(III), generally formed precipitates or jellies. Notable exceptions are the very stable and clear DMSO gels obtained after ca. 3 h from **3b**/Fe(III) and after 5 weeks from **3a**/Fe(III). The longer periods of time required for **3a** and **3b** to gelate DMSO may be due to the fast formation of weak DMSO–Fe(III) complexes that block somewhat formation of complexes with phosphonate headgroups.³³ Complexation of **5** by Fe(III) led to turbid gels in alcohols and low polarity and halogenated liquids. As noted,

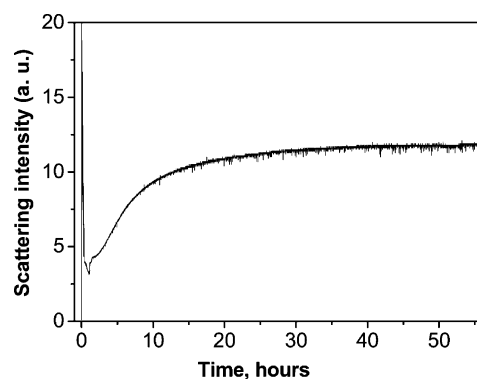


Figure 1. Scattering intensity changes with time upon gelation of 2 wt % **3b** in DMSO after addition of ca. 2 vol % MO-86.

some of the viscoelastic samples formed “jellies” (i.e., their yield stresses were sufficiently low such that some flow was noted when their tubes were inverted).

Gels of **7a**/Fe(III) were transparent in hydrocarbons and turbid or opaque in low polarity liquids. Pre-made Fe(III) complexes of **3**, **4**, and **10** were insoluble in hydrocarbon solvents even when heated, and the **6**/Fe(III) complex precipitated as a bulk solid when its hot solutions/sols were cooled. Gelation was improved slightly when the methoxy groups in **3b** were replaced with longer alkoxy groups, as in **5**. In several alcohols, complexes of **3–5** and **10** aggregated as inferred from the formation of jellies. As mentioned above, the viscosity of a 2 wt % **3b**/MO-86 solution/sol in DMSO slowly increased and a transparent gel was noted only after 3 h at room temperature. By contrast, the initial **3a**/MO-86 mixture in DMSO became a transparent gel only after standing at room temperature for 5 weeks!

In principle, the slow formation of the **3b**/MO-86 gels in DMSO offers an opportunity to investigate the mechanism of aggregation and SAFIN formation. Thus, gelation of **3b**/MO-86 in DMSO and **7a**/MO-86 in *n*-octane was monitored by a simple light scattering technique (Figure 1 and the Supporting Information, Figure 1). Immediately after the addition of MO-86 to both solutions, its color vanished and small amounts of precipitate (leading to very intense scattering until the particles settled) were noted. There was an appreciable increase in the viscosity of the solutions as well. The visual changes indicate that majority of the Fe(III) in MO-86 reacts very rapidly with phosphorus centers of **3b** and **7a** and leads to formation of aggregates. ¹H and ³¹P NMR spectra (Figures 2 and 3, respectively) of 1.8 wt % **3b** and in DMSO-*d*₆, recorded periodically after addition of 2.8 wt % MO-86, are consistent with the observations from light scattering measurements. The broadness and chemical shifts of the peaks indicate that most of the complexation of **3b** by the

(31) Lu, Q.; Ubillas, R. P.; Zhou, Y.; Dubenko, L. G.; Dener, J. M.; Litvak, J.; Phuan, P.-W.; Flores, M.; Ye, Z. J.; Gerber, R. E.; Truong, T.; Bierer, D. E. *J. Nat. Prod.* **1999**, *62*, 824–828.

(32) (a) Eldridge, J. E.; Ferry, J. F. *J. Phys. Chem.* **1954**, *58*, 992–995. (b) Raghavan, S. R.; Cipriano, B. H., chap 8 in ref 8c.

(33) Shvartsburg, A. A. *J. Am. Chem. Soc.* **2002**, *124*, 12343–12351.

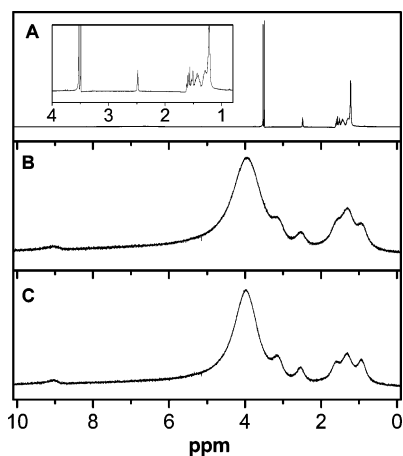


Figure 2. ^1H NMR spectra at room temperature of 1.8 wt % **3b** in $\text{DMSO-}d_6$ in the absence of MO-86 (A) and 3 min (B) and 60 min (C) after addition of 2.8 wt % MO-86 to the solution in A. The inset in A shows the expanded high-field portion of the **3b** resonances.

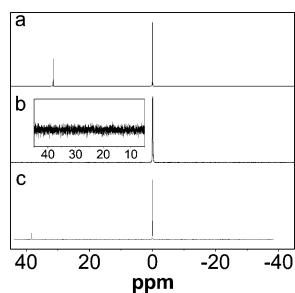


Figure 3. ^{31}P NMR spectra at room temperature of 2 wt % **3b** in $\text{DMSO-}d_6$ in the absence of MO-86 (a) and 3 min after addition of ca. 2 wt % MO-86 to the solution in panel a. ^{31}P NMR spectrum of a sol made from **7a**/ $\text{Al}(\text{iPrO})_3$ complex (0.14 wt %) in CDCl_3 is shown in panel c.³⁴ The peak at 0 ppm is from the reference, external phosphoric acid. The inset in panel b shows an expanded portion of the **3b**/Fe(III) spectrum where the resonance from **3b** is expected.

paramagnetic Fe(III) ions had already occurred after 3 min, even before there is an appreciable increase in solution/sol viscosity; additional analyses of these spectra will follow.

After an initial sharp increase, the scattering intensity of the sample containing **3b** rose slowly and achieved a plateau value after ca. 24 h. Good fits of the scattering profile required a multiexponential function, indicative of a complicated gelation mechanism. In agreement with our observations that gelation of **7a**/MO-86 in *n*-octane takes place almost immediately (i.e., no flow was observed a few seconds after addition of the MO-86), the initial scattering intensity from precipitates decreases sharply within the first few hours and then slowly decreases to a plateau value after ca. 10 h (Supporting Information, Figure 1). These data indicate that the initially formed aggregates redistribute themselves over time into more elongated objects; the kinetically formed and thermodynamically more stable objects are very different due to the mode by which the MO-86 is added.

As will be shown later, complexes prepared by adding 2 wt % MO-86 to a solution of 2 wt % **7a** in pentane, followed by evaporation of the pentane under a nitrogen stream with gentle warming, are organized in lamellae, whereas the aggregation of the complexes in the gels is in the form of inverted giant wormlike micelles (Figure 4). A DSC heating thermogram of the neat complex was featureless to 240 °C (Supporting Information, Figure 2); no endothermic peaks, indicative of melting of crystalline material, could be detected. Similarly, a heating thermogram of a gel prepared by adding 2 wt % MO-86 to a solution with 2 wt % **7a** in octane gave no indication of an

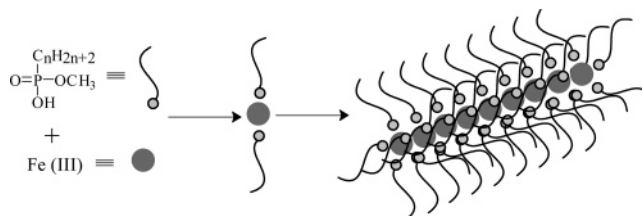


Figure 4. Cartoon representation of a giant wormlike micelle formed upon complexation of *n*-alkyl monophosphonate esters with Fe(III) ions. The gray spheres are phosphonate headgroups attached to a long alkyl chain and metal ions are the red spheres.

endotherm to >110 °C (Supporting Information, Figure 3), a temperature near to, but below, the boiling point of octane, 125 °C (and higher than the T_g values found for this gel using the inverted test tube method;³² Table 1), and an optical micrograph of the gel (Supporting Information, Figure 4) was not birefringent. On these bases, we conclude that packing of these complexes in gel aggregates is not crystalline, and in the neat material, it is a very disordered solid. In fact, it is known that some SAFINs are composed of amorphous fibers and others are crystalline,⁸ and that even one gelator may change from amorphous to crystalline depending on the liquid component.³⁵

Although the bolaamphiphile **3–5**/Fe(III) complexes are much less efficient gelators than the monophosphonate ester **7a**/Fe(III) complex, we attempted to strengthen the gelator networks of the monophosphonates by introducing “cross-links” comprised of a few bisphosphonate molecules that might span two fibers. However, addition of even small amounts of one of **3–5** decreased the gelation ability of **7a** in hydrocarbon liquids after addition of MO-86. These results indicate that the spacer lengths of the bisphosphonates are too short to extend beyond one inverse, rodlike micelle (vide infra). Also, addition of small amounts of **7a** did not improve the efficiency of gelation by **3–5**/Fe(III) complexes.

Comparisons between the gelation efficiency of the Fe(III) complexes of **7a** and those of **7b** and **9** allow the effects of adding more functional groups and introducing small structural modifications (N. B., shortening the long alkyl chain) to be explored. The gelation efficiency of iron complexes of methyl *n*-alkylphosphonates does not vary substantially as a function of alkyl chain length as long as the complex remains soluble in a hydrocarbon liquid.^{30c} Also, as indicated by the results in Table 2, substitution of a methoxyethyl moiety for the methyl ester group of **7a** (as well as the innocuous truncation of the long alkyl chain to tetradecyl), yielding **9**, does not change appreciably the gelation efficiency of the Fe(III) complexes (Table 2). However, introduction of an OH group at the end of the long alkyl chain (**7b**) does reduce its gelation efficiency dramatically; fewer liquids are gelled by the **7b**/Fe(III) complex, and the gels that do form persist for shorter periods at room temperature than those lacking an OH group at the end of the alkyl chain.

The effect of concentration on the gelation ability of the **7a**/MO-86 complex has been studied in three different liquids (Table 3). The results show that the extent of increase of T_g with concentration depends on the nature of the liquid. They indicate that solubility of the complex in the liquid and, perhaps, the ability of the liquid to interact with the components of the complex may affect the gelation. There is ample precedent for the liquid component having an important influence on the properties of molecular organogels.⁸

(34) George, M.; Funkhouser, G. P.; Weiss, R. G. unpublished results.

(35) Jeong, Y.; Hanabusa, K.; Masunaga, H.; Akiba, I.; Miyoshi, K.; Sakurai, S.; Sakurai, S. *Langmuir* **2005**, *21*, 586–594.

Table 2. Appearance^a and Periods of Stability^b of Gels Prepared from ca. 2 wt % **7b or **9** and an Equal Amount of MO-86 in Different Liquids with T_g (°C) Values in Parentheses**

liquid	appearance (T_g , °C)	
	7b	9
hexane	P	CG (63–70) ^c
<i>n</i> -octane	P	CG (68–75) ^c
<i>n</i> -decane	P	CG (62–74) ^c
silicone oil	TG (33–45) ^d	P
methanol	P	P
ethanol	P	P
1-butanol	P	P
1-octanol	P	turbid soln.
benzyl alcohol	viscous soln.	P
DMSO	S	P
toluene	TG (31–40) ^d	TG (29–40) ^c
chlorobenzene	OG (35–46) ^d	jelly
CCl ₄	P	TG (30–43) ^c

^a P, Precipitate; CG, clear gel; TG, turbid gel; S, solution. ^b Stable at room temperature in a sealed vial for: ^c >16 months; ^d 1 week.

Table 3. Concentration Dependence of Gelation by **7a and Equal Weights of MO-86 in Selected Liquids^a**

wt % 7a	appearance ^b (T_g °C)		
	<i>n</i> -octane	toluene	chlorobenzene
0.25	CG (rt)	TG (28–49)	TG (rt)
0.5	CG (35–60)	TG (43–51)	TG (23–28)
1.0	CG (42–65)	TG (42–50)	TG (26–33)
2.0	CG (56–82)	TG (50–62)	TG (28–35)
3.0	CG (71–85)	TG (62–72)	TG (25–34)
4.0	CG (75–93)	TG (60–71)	TG (34–47)
5.0	CG (75–98)	TG (66–79)	TG (29–46)

^a The gels are stable for >6 months at room temperature in sealed vials. ^b CG, clear gel; TG, turbid gel.

Proposed Mechanism of Complexation with MO-86 and Structures of the Complexes. Previous reports have shown that complexation of molecules similar to phosphonate esters (**3**, **5**, **7**, and **9**) and phosphonic acids (**4a,b**) by MO-86 involves coordination of Fe(III) with the oxygen atoms attached to phosphorus.^{36,37} Spectroscopic measurements suggest that complexation in a 3:1 phosphonate ester/Fe(III) mixture involves a change in the coordination number of phosphorus from 5 to 4 and formation of three four-membered rings consisting of P–O–Fe–O bonds.³⁶ However, magnetic measurements on and solubility characteristics of these complexes are more consistent with eight-membered phosphonate bridges and four-membered chelate rings, depending on the reaction temperature (Figure 5).^{37,38} The complexes between **2**, **4**, or **6a** and MO-86 did not gelate any of the liquids that were gelated by the corresponding MO-86 complexes with a mono-ester (**3**, **5**, **7a**, or **9**). These results imply that the structures of the Fe(III) complexes with **2**, **4**, and **6a** are different. Gelation and NMR studies of a (diamagnetic) **7a**/Al(III) complex showed that its gelation ability is similar to that of the **7a**/Fe(III) complex and that the methoxy group on phosphorus is not removed during complexation.³⁴ Thus, it is reasonable to assume that complexation of **3**, **5**, **7a**, and **9** by MO-86 involves interaction of ferric ion with the unesterified oxygen atoms.

Furthermore, the broadening of the ¹H and ³¹P NMR signals noted in Figures 2 and 3 after addition of MO-86 to DMSO-*d*₆

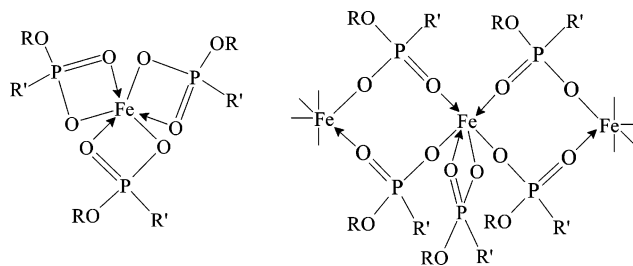


Figure 5. Two possible arrangements of the Fe(III) complex between phosphonate esters and the Fe(III) ions of MO-86.^{36a,37}

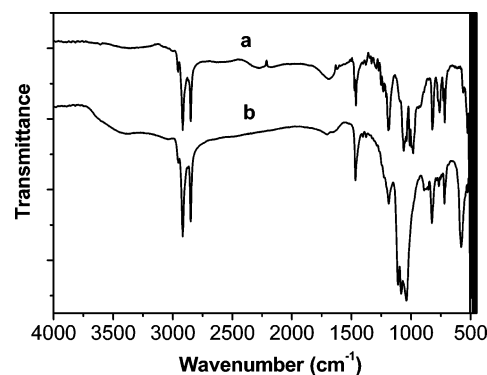


Figure 6. IR spectra of (a) solid **7a** and (b) its MO-86 complex.

solutions/sols of **3b** is due partially to the presence of the paramagnetic Fe(III) ions, whether complexed or free (Supporting Information, Figure 5). However, comparison of the degree of broadening for protons and phosphorus peaks indicates, as expected, that the Fe(III) ions reside in the proximity of the phosphorus atoms of **3b**. In support of this assertion, addition of one molar equivalent of the diamagnetic complexing agent, aluminum isopropoxide ((*i*PrO)₃Al), does not cause appreciable broadening of the ³¹P resonance of **7a** (Figure 3c).

The assumption that complexation of the phosphorus-containing latent gelators by MO-86 involves interaction of ferric ion with the unesterified oxygen atoms is supported by infrared spectroscopic investigations. The basic features of the IR spectra of neat **7a** and its Fe(III) complex are similar except between 1300 and 1000 cm⁻¹ and in the region centered at 3407 cm⁻¹ (Figure 6). However, no peak in the 1670–1600 cm⁻¹ region, corresponding to the bending modes of water,³⁹ is detectable in the spectrum of the complex. Therefore, the broad peak at 3407 cm⁻¹ in the complex is assigned to the stretching vibrations of the OH group attached to phosphorus. The IR spectrum of a *n*-decane gel containing 5 wt % **7a** and 5 wt % MO-86 (Supporting Information, Figure 6) has broad peaks at 3368 and 1639 cm⁻¹. They are assigned to the stretching and bending modes of water molecules. Furthermore, both the neat complex and its aggregates in the gel appear to have the same structure as indicated by the peaks in the 1200–1000 cm⁻¹ region.

Complexation of phosphonic acids with different metal cations has been studied recently, as well.^{9g,40,41} The 1:2.5 Fe(III): methylphosphonic acid (CH₃P(O)(OH)₂) complex has a layered structure with each Fe atom octahedrally coordinated to oxygen

(39) (a) Miller, F. A.; Wilkins, C. H. *Anal. Chem.* **1952**, *24*, 1253–1294. (b) Rao, C. N. R. *Chemical Applications of Infrared Spectroscopy*; Academic Press: New York, 1963; p 355.

(36) (a) Kokalas, J. J.; Kramer, D. N.; Block, F. *Spectrosc. Lett.* **1969**, *2*, 273–281. (b) Kokalas, J. J.; Kramer, D. N.; Temperley, A. A.; Levin, A. *Spectrosc. Lett.* **1969**, *2*, 283–287.

(37) Mikulski, C. M.; Karayannis, N. M.; Minkiewicz, J. V.; Pytlewski, L. L.; Labes, M. M. *Inorg. Chim. Acta* **1969**, *3*, 523–526.

(38) Grady, B.; Funkhouser, G. P. *J. Phys. Chem. B* submitted.

(40) (a) Yao, H.-C.; Li, Y.-Z.; Zheng, L.-M.; Xin, X.-Q. *Inorg. Chim. Acta* **2005**, *358*, 2523–2529. (b) Barja, B. C.; Herszage, J.; dos Afonso, M. S. *Polyhedron* **2001**, *20*, 1821–1830. (c) Nuernberger, M. Ger. Pat. # DE 19959592, 2001. *Chem. Abstr.* **2001**, *135*, 34900. (d) Altomare, A.; Bellitto, C.; Ibrahim, S. A.; Mahmud, M. R.; Rizzi, R. *J. Chem. Soc., Dalton Trans.* **2000**, 3913–3919. (e) Lacour, S.; Deluchat, V.; Bollinger, J.-C.; Serpaud, B. *Talanta* **1998**, *46*, 999–1009.

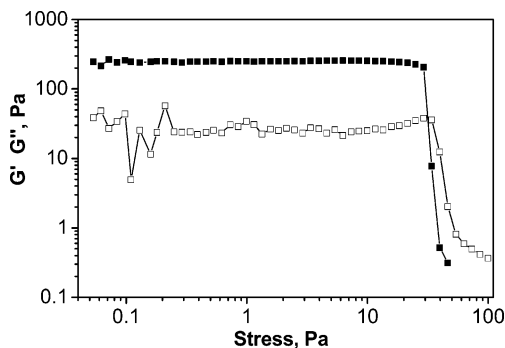


Figure 7. Elastic (G' , ■) and viscous (G'' , □) moduli at 25.0 °C versus shear stress (1 Hz constant frequency) of 2 wt % **3b** and 2 vol % of MO-86 in DMSO.

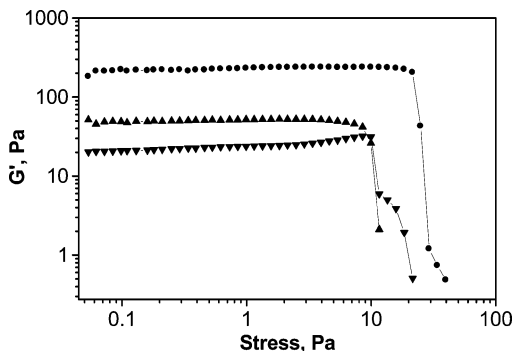


Figure 8. G' of 2 wt % **3a** in DMSO: 1 (▼), 2 (▲), and 5 days (●) after adding ca. 2 vol % MO-86.

atoms from six different molecules.⁴¹ Phosphate esters react with Al(III) cations to form structures with a center core surrounded by the alkyl chains.^{16c,42} A similar mechanism is proposed for the complexation of the bisphosphate ester **10** with Fe(III), in which three P–OH groups can react with one Fe(III). Although prepared by a different route, Kokalas et al. proposed the formation of an octahedral complex of iron with three phosphonate ester ligands.⁴³

Based on these studies and our own observations described above, we suggest that only two oxygen atoms of the phosphate diesters are involved in complexation with Fe(III),^{17,42a} complexation occurs very rapidly after addition of Fe(III), and aggregation of the complexes into inverted cylindrical micelles occurs more slowly (Figure 4).

Rheological Measurements. The qualitative measures of viscosities and viscosity changes mentioned above have been quantified by determining the rheological properties of gels consisting 2 wt % of a phosphorus-containing species, **3a,b** (in DMSO), **5** (in toluene), and **7a** (in *n*-dodecane), with ca. 2 wt % of MO-86 (Figures 7–9 and Supporting Information, Figures 7–11). Frequency sweeps were conducted at low shear strain, well within the linear viscoelastic (LVE) regime.⁴⁴ The data demonstrate that the samples are true gels⁴⁵ since G' (the elastic modulus) is always greater than G'' (the viscous component of

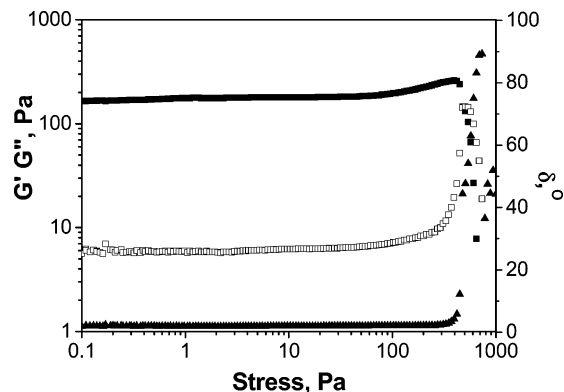


Figure 9. G' (■), G'' (□), and phase shift angle δ (▲) at 25.0 °C of 2 wt % **7a** and ca. 2 vol % MO-86 in *n*-dodecane versus shear stress (1 Hz constant frequency).

the modulus), and both are independent of frequency in the LVE regime.⁴⁶ The angles corresponding to the phase shifts, δ ($= \arctan(G''/G')$) of the gels (Supporting Information, Figures 9 and 11), are very low over a range of shear stress, indicative of a pronounced elastic (gel) nature. As indicated by the gels with **3a** and **3b** in DMSO, spacer length had a significant effect on the rate of gelation. By visual inspection and rheological measurements (Figure 7), gelation was rapid upon adding the Fe(III) source to the solution of **3b**. The shorter spacer length of **3a** dramatically lengthened the time required to form a gel despite the apparent very rapid complexation of Fe(III) by **3a** (vide ante). Over the course of 5 days, the initially very weak gel increased its strength to near that of the initial **3b**-based gel (Figure 8). Rapid gelation was also observed with **3b** in toluene, and **7a** in dodecane. These results, in combination with the light scattering studies, suggest that formation of the **3b**/Fe(III) complex and their aggregation into rodlike objects are diffusion and entropy controlled process.

The gel of the monofunctional gelator **7a** in dodecane had a lower elastic modulus than gels of the bolaamphiphilic gelators in DMSO and toluene, but the **7a** dodecane gel persisted to roughly an order of magnitude higher stress before breaking down. Thus, gels of the bolaamphiphiles also broke down at lower strains than the **7a** dodecane gel. Toluene gelled with **3b** had the highest storage modulus (~ 1500 Pa), but broke down at the lowest strain ($\sim 1\%$). DMSO gelled with either **3a** or **3b** failed at strains of 8–10%, but dodecane gelled with **7a** persisted to a strain in excess of 180%.

The increase of G' at high stress values noted in Figure 9 is likely a consequence of the cross-linked network structure within the gel. This allows the chains between junction zones, where chains are joined, to be stretched beyond their linear limit (strain hardening) before finally breaking at still higher stress (strain softening).⁴⁷

X-ray Diffraction Studies. Optical microscopy (vide infra) and small-angle X-ray scattering (SAXS) measurements of **3**/Fe(III) in DMSO gels or **7a**/Fe(III) in toluene or dodecane gels did not provide information consistent with the presence of a network of crystalline objects (Figure 10 and Supporting Information, Figure 12). The diffraction pattern of neat **7a**/Fe(III) contains fewer and broader peaks than that of neat **7a** (Figure

(41) (a) Palvadeau, P.; Queignec, M.; Venien, J. P. *Mater. Res. Bull.* **1988**, *23*, 1561–1573. (b) Sghyar, P. M.; Durand, J.; Cot, L.; Rafiq, M. *Acta Crystallogr.* **1991**, *C47*, 8–10. (c) Bujoli, B.; Palvadeau, P.; Rouxel, J. *Chem. Mater.* **1990**, *2*, 582–589. (d) Rao, B. V.; Palta, N.; Puri, D. M.; Sharma, N. D. *Transition Met. Chem.* **1988**, *3*, 281–283. (e) Gibson, D. H.; Ong, T. S.; Ye, M.; Franco, J. O.; Owens, K. *Organometallics* **1988**, *7*, 2569–2570.

(42) Similar structures have been reported for the Al(III) complexes of structurally related phosphate esters.^{17,22k}

(43) Kokalas, J. J.; Kramer, D. N.; Block, F. *Spectrosc. Lett.* **1969**, *2*, 273–281.

(44) Khan, S. A.; Royer, J. R.; Raghavan, S. R. *Aviation Fuels with Improved Fire Safety: A Proceeding*; National Academy Press: Washington, DC, 1997; pp 31–46.

(45) Although the magnitudes and ratios of the elastic (G') and loss (G'') moduli from rheological measurements provide a much more reliable viscoelastic distinction between a viscous sol and a gel, the “inverse flow” method³² was used to obtain approximate gelation temperatures.

(46) Lortie, F.; Boileau, S.; Bouteiller, L.; Chassenieux, C.; Demé, B.; Ducouret, G.; Jalabert, M.; Lauprêtre, F.; Terech, P. *Langmuir* **2002**, *18*, 7218–7222.

(47) Pellens, L.; Corrales, R. G.; Mewis, J. J. *Rheol.* **2004**, *48*, 379–393.

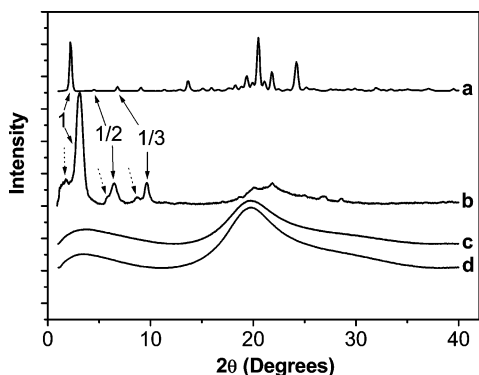


Figure 10. X-ray diffraction patterns at room temperature of neat **7a** (a), its Fe(III) complex (b), a *n*-dodecane gel of 2 wt % **7a** and ca. 2 wt % MO-86 (c), and neat *n*-dodecane (d). Data collection times are 1 (a, b) and 12 h (c, d). The diffractions from lamellae are indicated by solid arrows and other diffractions of the complex by dotted arrows.

10, diffractograms a and b), and no peaks were detectable in the gel diffractogram after protracted data collection (Figure 10c). Although the data indicate decreased crystallinity of the complex, the attenuation of clear diffraction peaks may also be interpreted as a consequence of very small crystalline aggregates, especially in the gel. We favor the former explanation based on the total body of experiments (N. B., the nonbirefringent appearance by polarizing optical microscopy (Supporting Information, Figure 4) and the lack of endothermic peaks in a DSC heating thermogram of a **7a**/Fe(III) gel in octane (Supporting Information, Figure 3)) and the consequences of formation of polymeric products associated with complexation.³⁷ In analogous experiments with the same concentration of very different gelators, we have been able to detect easily diffraction peaks from crystalline networks.⁴⁸

The reciprocal indices of the low angle peaks in the diffractograms of both **7a** and its complex indicate lamellar packing arrangements. The sequence of reciprocal spacings are 1, $1/2$, $1/3$, $1/4$, etc. for **7a** and its MO-86 complex (N. B., solid arrows in Figure 10). As indicated by the dotted arrows, the complex gives rise to other diffraction peaks that do not follow a recognizable sequence. Regardless, the X-ray data indicate the presence of more than one type of complex in the solid, and the broader peaks of the complex suggest more disperse ordering of them or small crystalline objects than in the neat solid of **7a**. Similar diffraction patterns have been observed for the **7a**/Al(III) complex.³⁴ From the Bragg relationship, the layer spacing (*d*) of a lamella of **7a** is 38.8 Å, about 1.5 times the calculated extended molecular length (26.7 Å⁴⁹). Two of the possible arrangements are partial interdigitation of (nearly) extended molecules in orthogonally packed layers or tilted, extended molecules within noninterdigitated layers. The observed lamellar thickness of **7a**/Fe(III), 26.7 Å, requires that its complex be packed as extended molecules in noninterdigitated, orthogonally packed layers.

Small Angle Neutron Scattering (SANS) Measurements. SANS studies of the **7a**/Fe(III) complex in gels with perdeuterated *n*-dodecane and perdeuterated toluene were conducted to determine the structures in the nanoscale involved in the networks.

(48) See for example: (a) George, M.; Tan, G.; John, V. J.; Weiss, R. G. *Chem. Eur. J.* **2005**, *11*, 3243–3254. (b) George, M.; Weiss, R. G. *Langmuir* **2003**, *19*, 1017–1025. (c) George, M.; Weiss, R. G. *Chem. Mater.* **2003**, *15*, 2879–2888. (d) Ostuni, E.; Kamaras, P.; Weiss, R. G. *Angew. Chem., Int. Ed.* **1996**, *35*, 1324–1326.

(49) Calculated by Hyperchem (version 7.1) molecular modeling system at the PM3 level, adding the van der Waals radii^{49a} of the terminal atoms. (a) *Lange's Handbook of Chemistry*, 13th ed.; Dean, A. J., Ed.; McGraw-Hill: New York, 1985; Sect. 3, pp 121–126.

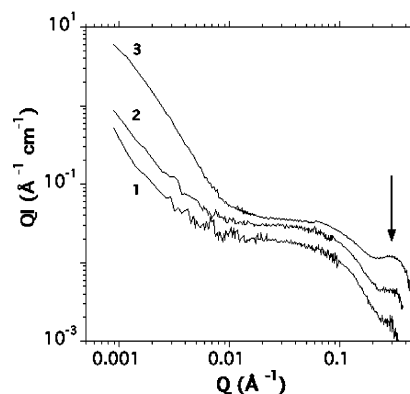


Figure 11. Holtzer representations of scattering data at 24 °C for gels consisting of (1) 2.07 wt % **7a**/MO-86 in toluene-*d*₈ and 2.9 wt % D₂O, (2) 1.0 wt % **7a**/MO-86 in toluene-*d*₈ and 1.9 wt % D₂O, and (3) 1.0 wt % **7a**/MO-86 in *n*-dodecane-*d*₂₆ and 9 wt % D₂O. SANS experiments were performed using preformed **7a**/MO-86 complex (see the Experimental Section) and the wt % given are those of the complex.

This information is necessary to complete the picture obtained at the molecular scale from the X-ray diffraction experiments. To minimize the concentrations of H atoms in the system, samples were prepared by adding various amounts of D₂O to mixtures of dried (see the Experimental Section) **7a**/Fe(III) complex in one of the perdeuterated liquids; no gel formed in the absence of water. Dissolution of the neat gelators led to heterogeneous gels, presumably due to inhomogeneous distribution of the D₂O; to avoid possible changes to the complexes, the samples were not heated and cooled to increase homogeneity prior to obtaining the SANS data.

Figure 11 shows the scattering curves for 3 gels in a Holtzer representation that conveniently reveals a “plateau-like” regime of the intensity decay within one decade of the intermediary *Q* range ($0.007 \text{ \AA}^{-1} < Q < 0.07 \text{ \AA}^{-1}$). This is a strong indication that this part of the scattering is attributable to the presence of long and rigid fibers in the gels. The profile of the curve at larger *Q*, with a sharp decay and a broad oscillation, are consistent scattering features typical of fibrillar scatterers.⁵⁰ The scattering function (eq 1) for cylindrical fibers (length *L*, radius *R*, and neutron volume contrast $\Delta\rho$; J_1 is the first order Bessel function of the first kind) qualitatively reproduce the 3 above-mentioned scattering features.

$$I(Q) = \frac{\pi L}{Q} \left[\pi R^2 \Delta\rho \frac{2J_1(QR)}{QR} \right]^2 \quad (1)$$

The sharp and intense very low-*Q* component reveals the presence of large-scale heterogeneities in the gel networks; they are expected based on the mode of gel preparation described above. Comparisons of curves 1 and 3 show that the volume fraction of such heterogeneities are significantly larger in the deuterated dodecane than in the deuterated toluene gels. The favorable *Q*-separation that allows the distinction between two structural components of the network architecture is assumed to be a consequence of the small cross-sectional dimensions of the fibers. The *Q*-separation in the scattering curve between the form-factor signal attributed to the fibers and the low-*Q* extra-intensity attributed to the heterogeneities is assumed to be due to the small cross-sectional dimensions of the fibers. This hypothesis is supported by the presence of an intensity oscillation (maximum at ca. 0.30 \AA^{-1}) and further Guinier analysis and fits (vide infra).

(50) Terech, P. In chapter 10 of ref 8c.

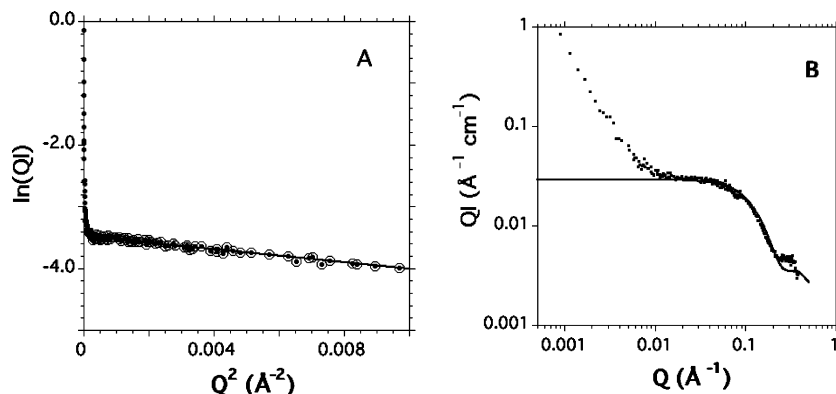


Figure 12. (A) Guinier plot of a gel consisting of 2 wt % **7a**/MO-86 complex in toluene- d_8 and 2.9 wt % D $_2$ O at 24 °C. From the slope of the linear part (excluding the very low- Q data due to the large-scale heterogeneities), a radius value $R = 14.6$ Å can be extracted using the equation, $I(Q) = \phi \pi/Q \Delta\rho^2 \pi r^2 \exp(-Q^2 R^2/4)$, that is valid at low Q values. (B) SANS data (dots) and a theoretical scattering function for cylindrical fibers with $R = 15$ Å (full line). A residual (0.5% of the signal amplitude at low Q) Lorentzian component centered at $Q \sim 0.325$ Å $^{-1}$ has been included (see text).

The diameter of the fibers has been extracted from a $\ln(QI)$ versus Q^2 Guinier plot (Figure 12A). Figure 12B, shows good agreement between the data and the theoretical scattering function for rigid cylindrical fibers of radius $R = 15$ Å (excluding again the lowest Q component). It confirms that the solidlike component of the gels is made up of long and rigid fibrillar species. The plateau and the sharp subsequent decrease in the QI versus Q curves are correctly reproduced by the fit as well as is the Q -position of the broad oscillation (at $Q \sim 0.30$ – 0.34 Å $^{-1}$) indicated by the arrow in Figure 11. To adjust the amplitude of the oscillation, a broad, underlying Lorentzian centered at $Q = 0.325$ Å $^{-1}$ must be introduced. It may indicate the presence of crystalline-like heterogeneities with poorly ordered periodicities in the 18–21 Å range. We repeat that such heterogeneities are not surprising given the method of sample preparation.

The distances calculated by X-ray diffraction for the neat complexes in lamellae and those from SANS for complexes in the gel are very different. Based on our calculation of the extended molecular length of **7a**, 26.7 Å, a diameter of ~ 30 Å (from SANS) requires that the long alkyl chains of molecules of Fe(III)-complexed **7a** be in extensively bent conformations if packing is like that in a “normal” inverted wormlike micelle (i.e., with at least 2 molecules per cross-sectional unit) or there be only one molecule of **7a** per cross-section.⁵¹ Additionally, molecules of D $_2$ O and deuterated solvent may perfume the aggregates, thereby changing the apparent cross-sectional stoichiometry. Regardless, complexed **7a** is not in similar environments in its neat lamellar and gel phases.

Conclusions

The structural and rheologic properties of this two-component gelator system have been investigated in detail to determine the factors leading to efficient gelation. In addition, the dynamics of gelation have been used to elucidate the sequence of steps commencing with addition of Fe(III) ions to solutions/sols of one of the phosphorus-containing latent gelators and ending with formation of a self-assembled fibrillar network and gelation. The results indicate that formation of complexes is very rapid and is followed by their aggregation into inverted giant rodlike micelles with narrow cross-sections; the neat complexes appear

to prefer to organize into lamellae. Several interesting features of the dependence on gel stability have been discovered by investigating the relationships between (1) structural and rheological properties of the gels and (2) the nature of the liquid component and the molecular structure of the phosphorus-containing latent gelator. They allow the design of gels of this class with specific properties. For instance, Fe(III) complexes of bisphosphonates **3a** and **3b** (differing only in the length of the methylene chain separating their phosphorus centers) require five weeks and ca. 3 h, respectively, to form a clear gel in DMSO that is stable at room temperature. However, once formed, the gels have comparable thermal stability. Also, the gels formed from Fe(III) complexes of the bisphosphonates **3a** or **3b** in DMSO and the monophosphate **7a** in *n*-dodecane are mechanically more stable to stress than that of toluene gels of the bisphosphonate **5** in which the spacer is the same length as in **3b** but the alkoxy chains are much longer and comparable to that in **7a**. Although these comparisons are not completely direct, they demonstrate that the properties of the gels can be modulated by careful choice of the structural variables in the phosphorus-containing latent gelators.

In fact, some of these complexes have already found uses in hydraulic fracturing^{30a,c} and we expect that they will have a variety of other applications as well. Most importantly, the results presented here provide an interesting study of the interplay between molecular structure, molecular complexation, self-assembly, and modulation of the macroproperties of the phases derived therefrom.

Acknowledgment. The Georgetown group thanks Halliburton Energy Services, Duncan, OK, and the National Science Foundation for their financial support. We thank The National Institute of Standards and Technology, U.S. Department of Commerce, for providing the neutron research facilities used in this work and the CNRS of France for a binational travel grant to P.T. This article is dedicated to Prof. Silvia E. Braslavsky on the occasion of her upcoming important birthday and retirement from the Max-Planck-Institut für Bioorganische Chemie (formerly Strahlenchemie).

Supporting Information Available: Spectroscopic and analytical data for new phosphonate esters and phosphinic acids, light scattering data, optical micrographs, DSC thermograms, rheology data, and NMR and IR spectra and XRD patterns of several gels and neat powder samples. This material is available free of charge via the Internet at <http://pubs.acs.org>.

(51) As an example, we take the 2 wt % **7a**/MO-86 gel in toluene. Assuming a stoichiometry of C $_{17}$ H $_{37}$ O $_3$ PFe, a density of 1.1 g cm $^{-3}$, and no perfusion of solvent or water into the inverted rodlike micelles, the number of molecules per unit length of fiber is $nL = 0.30$. If a mean value for the axial stacking is ca. 4 Å, there are 1.2 molecules per cross-sectional unit. Assuming a density of 1.2 g cm $^{-3}$, there are 1.44 molecules calculated per cross-sectional unit.